II International Conference on Simulation for Additive Manufacturing - Sim-AM 2019
F. Auricchio, E. Rank, P. Steinmann, S. Kollmannsberger and S. Morganti (Eds)

A NUMERICAL MODEL FOR THE SIMULATION OF SHALLOW LASER SURFACE MELTING

Alexandre Caboussat[*,a], Julien Hess[a,b], Alexandre Masserey[b] and Marco Picasso[c]

[a] Geneva School of Business Administration
University of Applied Sciences and Arts Western Switzerland (HES-SO)
Rue de la Tambourine 17, 1227 Carouge, Switzerland
e-mail: {alexandre.caboussat/julien.hess}@hesge.ch - web page: http://campus.hesge.ch/caboussat

[b] Ycoor Systems SA, Technopôle 10, 3960 Sierre, Switzerland
e-mail: {masserey/hess}@ycoorsystems.com - web page: http://www.ycoorsystems.com

[c] Institute of Mathematics, Ecole Polytechnique Fédérale de Lausanne (EPFL)
Station 8, 1015 Lausanne, Switzerland
e-mail: marco.picasso@epfl.ch - web page: https://people.epfl.ch/marco.picasso

Key words: Computational methods, Coupled problems, Marangoni effects, Operator splitting, Laser surface melting

Abstract. We present a multi-physics model for the approximation of the coupled system formed by the temperature-dependent Navier-Stokes equations with free surfaces. The main application is the industrial process of shallow laser surface melting (SLSM), for laser polishing of metal surfaces. We consider incompressible flow equations with solidification, and we model the laser source through physically-consistent boundary conditions. We incorporate Marangoni effects in the surface tension model to drive internal motion in the liquid metal. The numerical method relies on an operator splitting strategy and a two-grid approach. A proof of concept of the numerical model is achieved through a static laser melting process.

1 INTRODUCTION

Laser polishing is a widespread process in various industries [2, 14, 15], consisting in re-melting the surface of a metal in order to reduce surface roughness when re-solidifying. Its effectiveness relies on the strong dependency between the fluid flow properties of the metal (or alloy), and the heat effect [1]. The underlying multi-physics model for such a system is composed by the temperature-dependent Navier-Stokes equations, coupled with the heat equation for solidification processes, and with a free surfaces model for the simulation of the surface of the re-melting metal. Although no substrate is incorporated into the mixture here, the goal of this study is to simulate the internal motion of the melting pool, and accurately model the free surfaces that arise in laser polishing processes. In particular, we model the complex relationship between internal currents in the liquid metal, the temperature and the free surface evolution through Marangoni effects [5, 13]. The objective of this work is thus to highlight the internal fluid motion induced by Marangoni effects in laser surface melting processes.

We consider incompressible flow equations with solidification, by using a Navier-Stokes model with an additional Carman-Kozeny term [9]. We add thermal effects with an enthalpy-based convection-diffusion heat equation, and we model the laser source by applying a heat flux boundary condition on the free surface. We incorporate Marangoni effects in the surface tension model to drive internal motion in the liquid metal. The numerical method relies on an operator splitting strategy and a two-grid approach, which has been tested in other situations (without solidification effects) in [3, 4, 6]. The operator splitting allows to decouple the various physical phenomena, in particular advection and diffusion processes. The two-grid approach allows to have an accurate description of the free surfaces.

A proof of concept of the numerical approach is achieved through an example of static laser melting, to show how laser polishing processes can induce convective currents in the melting regions, through Marangoni effects, and affect surface roughness.

2 MODELING

Let us consider a bounded domain $\Lambda \subset \mathbb{R}^3$, and let $t_{max} > 0$ be a given final time. For any time $t \in (0, t_{max})$, let $\Omega_t \subset \Lambda$ be the domain occupied by the metal (solidified or not) and $\Gamma_t := \partial\Omega_t \backslash \partial\Lambda$ be the free surface between the metal and the ambient air, namely the boundary of the metal domain that is not in contact with the boundary of the whole cavity. The air is considered as vacuum. Typically, we consider the laser polishing of a metal plate Ω_t, as illustrated in Figure 1 in two space dimensions.

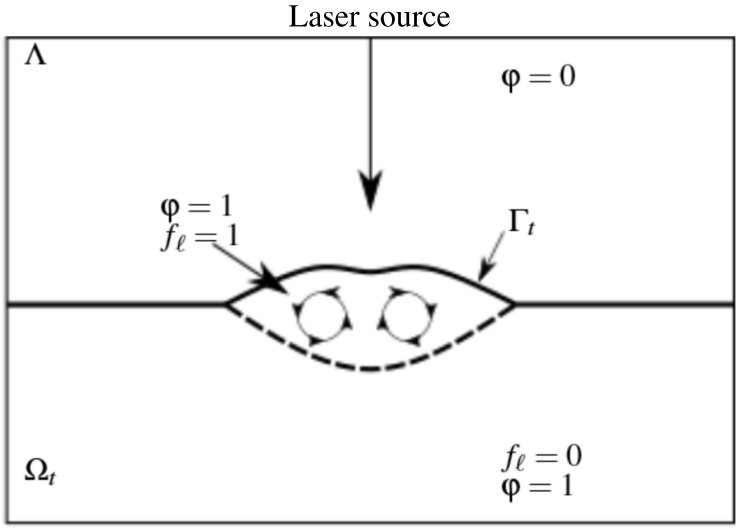

Figure 1: Laser melting of a metal plate (2D sketch). The cavity Λ contains metal and air. At each time $t \in (0, t_{max})$, the metal domain Ω_t (solid and liquid) is separated from the ambient air by the metal-air interface Γ_t. A vertical laser source is applied in the middle of the domain and melts the central region of the metal. A vorticity flow develops in the liquid region. The metal domain is described by its volume fraction of metal φ, while the temperature T determines the liquid and solid regions.

Let Q be the space-time domain containing the metal:

$$Q = \{(\mathbf{x},t) \in \Lambda \times (0,t_{max}) : \mathbf{x} \in \Omega_t, 0 < t < t_{max}\}.$$

The velocity field $\mathbf{v} : Q \to \mathbb{R}^3$ and the pressure field $p : Q \to \mathbb{R}$ are assumed to satisfy incompressible, time-dependent Navier-Stokes equations in Q. The Navier-Stokes equations include an additional Darcy-like reaction term to model the solidification process, penalizing the velocity in the solid region. The enthalpy $H : Q \to \mathbb{R}$ is assumed to satisfy the classical enthalpy formulation of the heat conservation equation, which can be derived by simplifying the general energy conservation equation with Fourier's law (see [9] for details). The complete set of equations in Q thus reads:

$$\rho \frac{\partial \mathbf{v}}{\partial t} + \rho(\mathbf{v} \cdot \nabla)\mathbf{v} - 2\nabla \cdot (\mu \mathbf{D}(\mathbf{v})) + \alpha(T)\mathbf{v} + \nabla p = \rho \mathbf{g}, \tag{2.1}$$

$$\nabla \cdot \mathbf{v} = 0, \tag{2.2}$$

$$\frac{\partial H}{\partial t} + \mathbf{v} \cdot \nabla H - \nabla \cdot (k \nabla \beta(H)) = 0. \tag{2.3}$$

Here $\mathbf{D}(\mathbf{v}) = 1/2\,(\nabla \mathbf{v} + \nabla \mathbf{v}^T)$ is the symmetric deformation tensor, ρ, μ and k are respectively the density, the viscosity and the thermal conductivity of the metal, and $\rho\mathbf{g}$ is the gravity force. The function $T = \beta(H)$ describes the relationship between the enthalpy H and the temperature T, and is determined by the phase transition and properties of the material.

In order to model the solidification process with a diffuse model (mushy zone), the velocity is penalized with the Carman-Kozeny empirical law, which represents the coupling with a Darcy flow in porous media [9]. The reaction coefficient in (2.1) is given by:

$$\alpha(T) = \bar{\alpha} \frac{\mu (1 - f_\ell(T))^2}{(f_\ell(T) + \varepsilon)^3}, \tag{2.4}$$

where $\bar{\alpha}$ is a constant to be calibrated and f_ℓ is the liquid fraction, which equals one in the liquid region (above the temperature of fusion) and zero in the solid region. Note that $0 < \varepsilon << 1$ is a numerical parameter to avoid a division by zero.

Let $\varphi : \Lambda \times (0,t_{max}) \to \{0,1\}$ be the volume fraction of metal, which equals one if the metal is present (solid or liquid) and zero if it is not (also known as the characteristic function of the metal domain), and thus the space-time metal domain can be defined as:

$$Q = \{(\mathbf{x},t) \in \Lambda \times (0,t_{max}) : \varphi(\mathbf{x},t) = 1\}.$$

In order to describe the kinematics of the free surface, the volume fraction of metal φ must satisfy (in a weak sense) the transport equation:

$$\frac{\partial \varphi}{\partial t} + \mathbf{v} \cdot \nabla \varphi = 0 \qquad \text{in } \Lambda \times (0,t_{max}), \tag{2.5}$$

The model is completed with initial and boundary conditions. The volume fraction of metal $\varphi(\cdot,0)$ is given at initial time, which is equivalent to defining the initial metal region $\Omega_0 = \{\mathbf{x} \in \Lambda : \varphi(\mathbf{x},0) = 1\}$. The initial enthalpy (or equivalently temperature), and velocity fields are then prescribed in Ω_0. Boundary conditions for φ are applied, if necessary, on the inlet part of $\partial\Omega_t$ for (2.5). The Navier-Stokes equations (2.1)-(2.2) are completed with slip or no-slip boundary conditions imposed on the boundary of the metal domain $\partial\Omega_t$ that is in contact with the boundary of the cavity $\partial\Lambda$.

Surface tension and Marangoni effects on the liquid metal-air interface are taken into account via a force term on the free surface [13]. The ambient air is assumed to have no influence on the metal, and is treated as vacuum. The boundary conditions on the metal-air interface are thus given by:

$$-p\mathbf{I} + 2\mu\mathbf{D}(\mathbf{v}) = \gamma\kappa\mathbf{n}_{\Gamma_t} + \nabla_{\Gamma_t}\gamma, \qquad \text{on} \quad \Gamma_t = \partial\Omega_t \backslash \partial\Lambda, \tag{2.6}$$

where $\mathbf{n}_{\Gamma_t}$ is the external unit normal vector to Γ_t towards the vacuum, κ is the curvature of Γ_t, and γ is the surface tension coefficient. In the sequel, we'll assume that $\gamma = \gamma(T)$ only depends on the temperature. In this case, the term $\nabla_{\Gamma_t}\gamma$ is defined as $\nabla_{\Gamma_t}\gamma = \gamma'(T)\nabla T \cdot \mathbf{t}_1 + \gamma'(T)\nabla T \cdot \mathbf{t}_2$, where $\mathbf{t}_i$, $i = 1,2$, are two linearly independent vectors in the plane tangent to Γ_t, and perpendicular to $\mathbf{n}_{\Gamma_t}$. [1]

The boundary conditions for the heat equation (2.3) are as follows: the laser source is modeled via a given heat flux on the boundary Γ_t of the metal domain, while adiabatic boundary conditions are applied on the rest of the boundary.

The coupled multiphysics problem thus consists in finding the time evolution of the position of the volume fraction of metal φ in the cavity Λ, together with the enthalpy H, the velocity $\mathbf{v}$ and the pressure p in the metal domain only.

3 NUMERICAL METHODS

The numerical method is inspired from [3, 4, 6], where it has been validated in various situations. It is adapted here to the coupled multi-physics problem arising when considering temperature-related effects. It relies on *operator splitting* and a *two-grid* method: the splitting algorithm decouples advection and diffusion phenomena, while the two-grid algorithm allows to increase the accuracy of the approximation of the free surface by considering finer grids for the approximation of advection problems.

3.1 Time splitting algorithm

Let $N \in \mathbb{N}$, and $\tau = t_{max}/N$ a constant time step. A subdivision of the time interval $[0, t_{max}]$ is given by $t^n = n\tau$, $n = 0, \ldots, N$. Assume that φ^n is an approximation of φ available at time t^n, which defines the metal domain $\Omega^n = \{\mathbf{x} \in \Lambda : \varphi^n(\mathbf{x}) = 1\}$, and that $\mathbf{v}^n, p^n, T^n, H^n$ are known approximations of $\mathbf{v}, p, T, H$ respectively on Ω^n at time t^n. Then the approximations φ^{n+1},

[1] Note that if γ is a function of $\mathbf{x} \in \mathbb{R}^3$, the operator ∇_{Γ_t} is the surface gradient for the surface Γ, and is defined by $\nabla_\Gamma\gamma := \nabla\gamma - \mathbf{n}_\Gamma(\mathbf{n}_\Gamma \cdot \nabla\gamma)$.

Ω^{n+1}, $\mathbf{v}^{n+1}$, p^{n+1}, T^{n+1}, H^{n+1} at time t^{n+1} are computed by means of a splitting algorithm as illustrated in Figure 2.

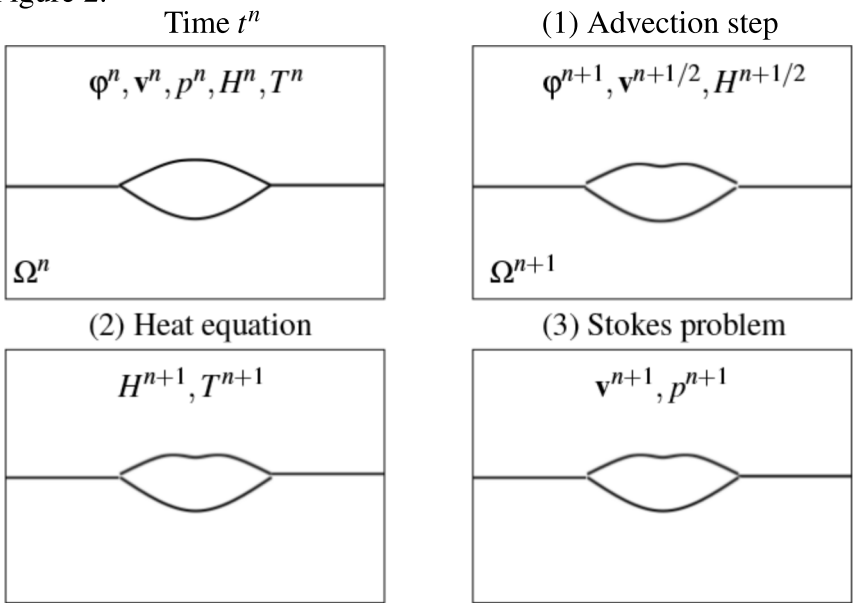

Figure 2: Operator splitting algorithm (from left to right, top to bottom). We solve successively (1) Three advection problems in order to obtain $\varphi^{n+1}, \mathbf{v}^{n+1/2}, H^{n+1/2}$ and thus Ω^{n+1}. (2) The heat diffusion equation (without convection) to determine H^{n+1} (and thus T^{n+1}). (3) A generalized Stokes problem in order to obtain $\mathbf{v}^{n+1}$ and p^{n+1}.

3.1.1 Advection equations

First, three advection problems are solved in order to obtain the new volume fraction of metal φ^{n+1} (and thus the new metal domain Ω^{n+1}), the predicted velocity $\mathbf{v}^{n+1/2}$ and the predicted enthalpy $H^{n+1/2}$. In order to do so, the advection operators in (2.1), (2.3) and (2.5) are solved in Λ between t^n and t^{n+1}:

$$\frac{\partial \varphi}{\partial t} + \mathbf{v} \cdot \nabla \varphi = 0, \qquad \frac{\partial H}{\partial t} + \mathbf{v} \cdot \nabla H = 0, \qquad \frac{\partial \mathbf{v}}{\partial t} + (\mathbf{v} \cdot \nabla)\mathbf{v} = \mathbf{0}, \tag{3.1}$$

with initial conditions provided by φ^n, H^n and $\mathbf{v}^n$ respectively. This system of hyperbolic equations is linearized and solved with a forward characteristics method [6], which reads:

$$\varphi^{n+1}(\mathbf{x} + \tau \mathbf{v}^n(\mathbf{x})) = \varphi^n(\mathbf{x}), \quad H^{n+1/2}(\mathbf{x} + \tau \mathbf{v}^n(\mathbf{x})) = H^n(\mathbf{x}), \quad \mathbf{v}^{n+1/2}(\mathbf{x} + \tau \mathbf{v}^n(\mathbf{x})) = \mathbf{v}^n(\mathbf{x}),$$

for all $\mathbf{x} \in \Lambda$. The new metal domain is then defined as $\Omega^{n+1} = \{\mathbf{x} \in \Lambda : \varphi^{n+1}(\mathbf{x}) = 1\}$.

3.1.2 Heat equation

Then the heat equation (without convection term) allows to determine the corrected enthalpy H^{n+1} in the new metal domain Ω^{n+1} by solving:

$$\frac{\partial H}{\partial t} - \nabla \cdot (k \nabla \beta(H)) = 0, \tag{3.2}$$

with initial conditions provided by $H^{n+1/2}$. We use an implicit Euler scheme with appropriate boundary conditions, together with the implicit enthalpy-temperature relation $T^{n+1} = \beta(H^{n+1})$ for the determination of the new temperature T^{n+1}. This time-discretized system of equations is solved with the so called Chernoff numerical scheme [10].

3.1.3 Stokes equations

Finally, a generalized Stokes problem is solved in order to obtain the corrected velocity $\mathbf{v}^{n+1}$ and pressure p^{n+1} in the new metal domain Ω^{n+1}, by solving:

$$\rho \frac{\partial \mathbf{v}}{\partial t} - 2\nabla \cdot (\mu \mathbf{D}(\mathbf{v})) + \alpha(T^{n+1})\mathbf{v} + \nabla p = \rho \mathbf{g}, \tag{3.3}$$

$$\nabla \cdot \mathbf{v} = 0. \tag{3.4}$$

An implicit Euler scheme is used for the time discretization of this Stokes system in Ω^{n+1}, together with the natural force condition on the metal-air interface:

$$-p\mathbf{I} + 2\mu \mathbf{D}(\mathbf{v}) = \gamma(T^{n+1})\kappa \mathbf{n}_{\Gamma^{n+1}} + \nabla_{\Gamma^{n+1}} \gamma(T^{n+1}), \quad \text{on } \Gamma^{n+1}. \tag{3.5}$$

3.2 Space Discretization

In order to solve this multi-physics problem, a two-grid method is used, following [3, 4, 6]. As illustrated in Figure 3 (in two dimensions of space), a regular grid of small structured cells (with typical cell size h_{cells}) is used to solve the advection problems (3.1), while the solutions of the heat problem (3.2) and of the Stokes problem (3.3)-(3.5) are obtained via a finite element approximation on a coarser unstructured tetrahedral finite element mesh (with typical mesh size h_{fe}).

The initial goal of introducing a two-grid method is to increase the accuracy of the approximation of the free surface (by decreasing the numerical diffusion of the approximation φ^{n+1} in (3.1)), while keeping reasonable the computational cost of solving parabolic problems (incl. the Stokes problem) implicitly. Following [6], we typically advocate $h_{fe} \simeq 3h_{cells}$ for a reasonable trade-off between accuracy and computational efficiency.

More precisely, (3.1) is solved with a *forward characteristics method* on the grid of small cells, together with a SLIC interface reconstruction algorithm for the approximation of φ^{n+1} [7],

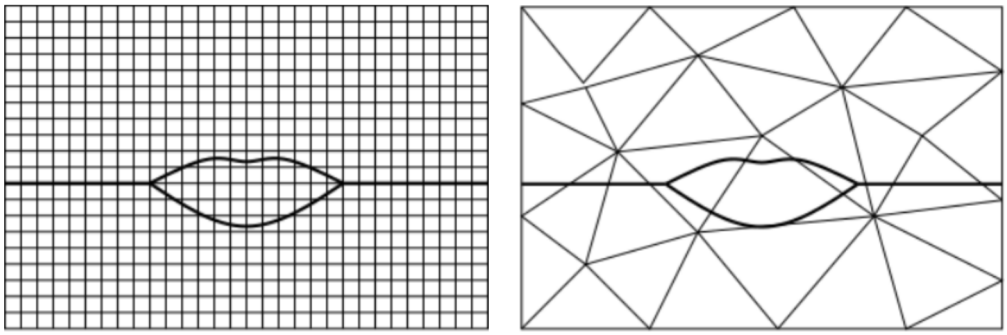

Figure 3: Two-grid method (2D sketch). The advection problems are solved on a structured grid of small cubic cells of typical size h_{cells} (left), and the diffusion problems are solved on an unstructured finite element mesh of typical size h_{fe} (right).

and post-processing heuristics to avoid artificial compression. Although the forward characteristics method does not have to satisfy a CFL condition theoretically, the time step τ is chosen in order to control the CFL number (to be typically between 1 and 5).

Stabilized finite elements, based on continuous piecewise linear finite elements, are used to approximate the Stokes problem (3.3)-(3.5), while classical continuous piecewise linear finite elements are used for the approximation of the heat equation (3.2).

4 NUMERICAL RESULTS

In order to illustrate the efficiency of our method, we present one numerical experiment that consists of a single static laser source melting a piece of metal. This experiment was also treated in [12], and first reported in [8]. We consider the Böhler S705 steel, whose physical properties are listed in Table 1. The variation of active elements, typically sulphur concentration in the material, affects the surface tension gradient with respect to the temperature, and as a consequence the direction and strength of the Marangoni convective flow and eventually the melting pool shape.

In addition to the physical properties in Table 1, the enthalpy-temperature relation $T = \beta(H)$ is constructed from ρ, C_{p_s}, C_{p_s}, T_f and L, as in [10]. The surface tension coefficient is constructed as $\gamma(T) = 1.943 + \gamma'(T)T$ [N/m], where the surface tension derivative $\gamma'(T)$ is given in Figure 4 for two sulphur contents (see [11] for more details). The numerical results presented here are obtained with the curve corresponding to 150 ppm.

The static laser source is considered as a beam of radius $R = 1.4$ [mm] with a power of $P = 5200$ [W]. The absorptivity of the surface to the laser is $\eta = 0.13$ [-]. We simulate the process during $t_{max} = 1$ [s].

We setup a pseudo-2D geometry as illustrated in Figure 5. The computational domain is $\Lambda = D_1 \cup D_2 \cup D_3$, with the initial metal domain $\Omega_0 = D_1 \cup D_2$. The bounding box of the whole domain is $(0,14) \times (0,0.05) \times (0,7.25)$ [mm]. The finite-element mesh in regions D_2 and D_3 is very fine to capture fluid motions in the melting pool, while D_1 is coarser. This allows

Properties	Values	Units
Density (ρ)	8100	[kg/m^3]
Temperature of fusion (T_f)	1620	[K]
Dynamic viscosity (μ)	0.006	[kg/(m.s)]
Thermal conductivity of solid (k_s)	22.9	[J/(m.s.K)]
Thermal conductivity of liquid (k_l)	22.9	[J/(m.s.K)]
Enhancement factor for viscosity and liquid thermal conductivity	7.0	[-]
Specific heat of solid (C_{p_s})	627	[J/(kg.K)]
Specific heat of liquid (C_{p_l})	723.14	[J/(kg.K)]
Latent heat of fusion (L)	2.508e+5	[J/kg]

Table 1: Material properties for Böhler S705 steel.

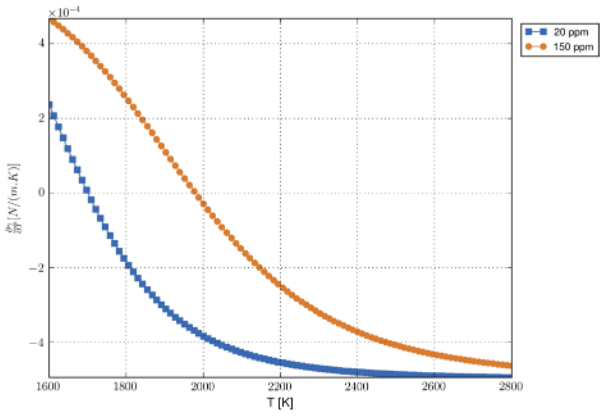

Figure 4: Surface tension derivative $\gamma'(T)$ as a function of temperature.

to decrease the computational time while keeping a good precision in the liquid metal. The discretization parameters are $\tau = 5 \cdot 10^{-5}$ [s], $h_{fe} = 5 \cdot 10^{-2}$ [mm], and $h_{cells} = 1.5 \cdot 10^{-2}$ [mm].

The laser source is modeled by a heat flux boundary condition (where heat loss is neglected). We assume that the flux distribution depends only on the distance r to the central point, and has the following profile:

$$k\frac{\partial T}{\partial n} = \begin{cases} \dfrac{C\eta P}{\pi R^2} & r \leq R \\ 0 & r > R \end{cases} \quad \text{on } \Gamma_t,$$

where $C = 0.2$ is a constant to account for the pseudo-2D approximation, η is the metal absorptivity, P is the laser power and R is the laser beam radius. Adiabatic boundary conditions are imposed on the rest of the boundary. The initial condition for the heat problem is the ambient temperature (no liquid region), and $f_\ell \equiv 0$ in Ω_0.

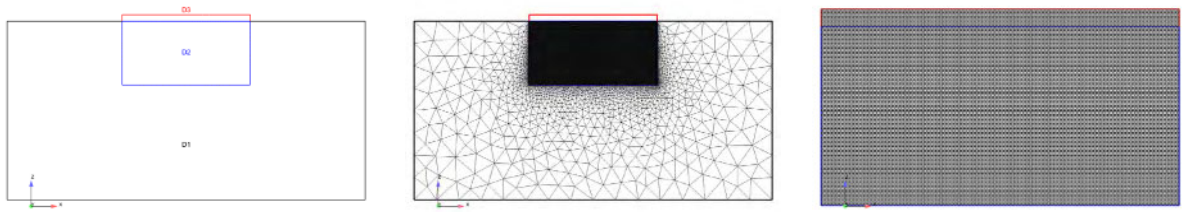

Figure 5: Static laser melting (2D sketch). Computational domains (left), finite element mesh (middle) and structured grid of small cells (right).

For the Stokes problem, we consider the gravity forces with $\mathbf{g}$ aligned with $\mathbf{e}_z$. The coefficients in the Carman-Kozeny term are given by $\bar{\alpha} = 100$ and $\varepsilon = 10^{-3}$. We apply slip boundary conditions in the xz-plane (pseudo-2D), no slip boundary conditions on $\partial\Lambda$ and the natural force conditions on the free surface Γ_t. The initial condition for the velocity is the zero velocity.

The laser source induces a heating effect that creates a liquid metal zone in the center of the metal domain. Marangoni effects generate a horizontal force at the liquid metal interface and set the fluid in motion. The internal currents induce a deformation of the free surface between the liquid metal and the ambient air.

Figure 6 illustrates the solution after $t = 1$ [s], namely the liquid fraction, the velocity field, the temperature and the shape of the free surface. Numerical experiments show a strong coupling between the thermal aspects and the deformation of the free surface.

5 CONCLUSIONS AND PERSPECTIVES

A set of equations has been presented to model melting metal with a free surface as it appears in laser surface melting processes. It allows to couple incompressible fluid flow equations with the heat equation and a free surface. A numerical model combining an operator splitting algorithm and a two-grid method has been used to test the model. Preliminary results have illustrated the coupling between the different physical phenomena (Marangoni effects, free surface evolution, melting zone). In particular, results have emphasized the strong effect of the varying temperature, due to laser processing, on the free surface and metal roughness.

6 ACKNOWLEDGMENTS

The authors thank B. Meylan, K. Wassmer, P. Hoffman (EMPA), E. Boillat (EPFL), I. Calderon and J.-C. Prélaz (Unitechnologies SA) for fruitful discussions. All the computations were performed using the software `cfsFlow++` developed by EPFL and Ycoor Systems SA.

REFERENCES

[1] E. Boillat, S. Kolossov, and R. Glardon. *Three dimensional FEM-simulation of the selective laser sintering process with locally renewed meshes and non-constant thermal con-*

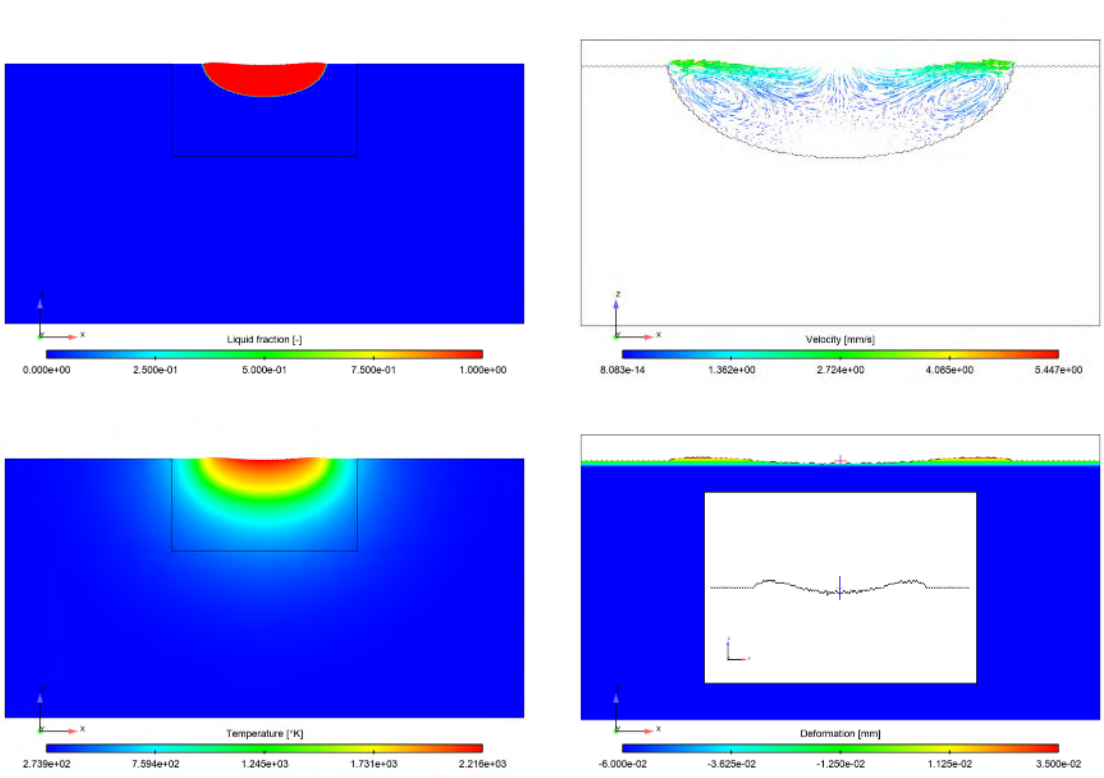

Figure 6: Static laser melting. Snapshots at time $t = 1\,[s]$, of the numerical approximation of: the liquid fraction f_ℓ (top left); the velocity field $\mathbf{v}$ (top right); the temperature T (bottom left); the deformation of the free surface Γ_t defined by the transport of φ (bottom right).

ductivity, pages 357–367. Proceedings of the 8th Solid Freeform Fabrication Symposium. 2002.

[2] E. V. Bordatchev, A. M. K. Hafiz, and O. R. Tutunea-Fatan. Performance of laser polishing in finishing of metallic surfaces. *Int. J. Adv. Manuf. Technol.*, 73(1-4):35–52, 2014.

[3] A. Caboussat. A numerical method for the simulation of free surface flows with surface tension. *Computers and Fluids*, 35(10):1205–1216, 2006.

[4] A. Caboussat, M. Picasso, and J. Rappaz. Numerical simulation of free surface incompressible liquid flows surrounded by compressible gas. *J. Comput. Phys.*, 203(2):626–649, 2005.

[5] D. Kothe, M. M. Francois, and J. M. Sicilian. Modeling of thermocapillary forces within a volume tracking algorithm. *Modeling of Casting, Welding and Advanced Solidification Processes - XI*, 2:935–942, 2006.

[6] V. Maronnier, M. Picasso, and J. Rappaz. Numerical simulation of three dimensional free surface flows. *Int. J. Num. Meth. Fluids*, 42(7):697–716, 2003.

[7] W. F. Noh and P. Woodward. SLIC (simple line interface calculation). *Proceedings of the Fifth International Conference on Numerical Methods in Fluid Dynamics*, 59:330–340, 1976.

[8] W. Pitscheneder, T. Debroy, K. Mundra, and R. Ebner. Role of sulfur and processing variables on the temporal evolution of weld pool geometry during multikilowatt laser beam welding of steels. *Welding research*, 75:71–80, 03 1996.

[9] M. Rappaz, M. Bellet, and M. Deville. *Modeling in Materials Science and Engineering*. Springer Series in Computational Mathematics. Springer Verlag, Berlin Heidelberg, 2003.

[10] Y. Safa, M. Flueck, and J. Rappaz. Numerical simulation of thermal problems coupled with magnetohydrodynamic effects in aluminium cell. *Applied Mathematical Modelling*, 33(3):1479 – 1492, 2009.

[11] P. Sahoo, T. Debroy, and M. J. McNallan. Surface tension of binary metal - surface active solute systems under conditions relevant to welding metallurgy. *Metallurgical Transactions B*, 19(3):483–491, 1988.

[12] Z. S. Saldi. *Marangoni driven free surface flows in liquid weld pools*. PhD thesis, Department of MultiScale Physics, Faculty of Applied Sciences, Delft University of Technology, Delft, The Netherlands., 2012.

[13] G. P. Sasmal and J. I. Hochstein. Marangoni convection with a curved and deforming free surface in a cavity. *Journal of Fluids Engineering*, 116(3):577–582, 1994.

[14] A. Temmler, E. Willenborg, and K. Wissenbach. Design surfaces by laser remelting. *Physics Procedia*, 12:419–430, 2011.

[15] A. Temmler, E. Willenborg, and K. Wissenbach. Laser polishing. *Proceedings of SPIE - The International Society for Optical Engineering*, 8243:19–, 02 2012.